Low-Complexity Sequential Information and Energy Reception

Sotiris A. Tegos*, Panagiotis D. Diamantoulakis*, Koralia Pappi†*, Paschalis C. Sofotasios‡§, Sami Muhaidat‡, and George K. Karagiannidis*
*Department of Electrical & Computer Engineering, Aristotle University of Thessaloniki, GR-54124 Thessaloniki, Greece
†Intracom S. A. Telecom Solutions, GR-57001, Thessaloniki, Greece
‡Center for Cyber-Physical Systems, Department of Electrical & Computer Engineering, Khalifa University, Abu Dhabi, UAE
§Department of Electrical Engineering, Tampere University, Tampere, Finland
e-mails: {tegosoti, padiaman, kpappi, geokarag}@auth.gr; {p.sofotasios, muhaidat}@ieee.org

***Abstract*—This contribution evaluates and optimizes the performance of simultaneous wireless information and power transfer (SWIPT) with an integrated energy and information receiver, which is characterized by low complexity and energy cost. To this end, a tractable expression for the achievable rate is derived, which is subsequently used to quantify the achievable harvested energy−rate region for the considered time-switching (TS) protocol. Sequential reception of energy and information can be implemented with the aid of TS, which also reduces complexity whilst it is useful in applications that the receiver does not have to be continuously active. In this context, the joint harvested energy−rate outage probability is also defined and minimized for a point-to-point and multicasting system, determining the optimal TS factor. Finally, respective computer simulations corroborate the effectiveness of the proposed framework, whilst interesting insights are developed which are expected to be useful in the design and effective operation of TS wireless power systems.**

I. Introduction

Emerging wireless technologies are largely characterized by versatile, yet stringent energy efficiency requirements of numerous involved devices. Therefore, wireless power transfer constitutes a promising paradigm as it can ultimately increase the efficiency and lifetime of such devices [1], [2]. This is particularly important in applications relating to the Internet-of Things (IoT), such as wearables and sensors networks, since energy harvesting (EH) can assist in achieving robust operation under realistic mobility requirements. This is, in fact, highly desirable since replacing or recharging the batteries of an increased number of devices is typically inconvenient, costly and even dangerous, particularly in remote areas, harsh industrial environments and healthcare applications.

Harvesting energy from sources that intentionally generate energy, such as radio frequency (RF) signals, turns out to be a more effective and interesting alternative. To this end, the potential to apply this concept, termed as wireless power transfer (WPT), in wireless communication applications has recently received considerable attention [2]. However, WPT creates unique challenges in the design of communication systems since, in some cases, it conflicts with the corresponding information transmission. More specifically, nodes cannot harvest energy and receive information simultaneously, which complicates the design of communication systems with WPT [1], [3]. This is the main challenge of simultaneous wireless information and power transfer (SWIPT), which aims at unifying the information and energy transmission by also taking into account the inherent dependence on specific system implementations [4], and the references therein. To achieve this in single-antenna nodes, two fundamental approaches have been proposed, namely the power-splitting (PS) strategy and the time-switching (TS) strategy [5]. In this context, the idea of SWIPT has been addressed in various investigations, such as multiple-input multiple-output (MIMO) communications [6], orthogonal frequency division multiplexing (OFDM) [7], cooperative networks [8] and physical layer security based wireless communications [9].

It is recalled that most contributions in the open literature focus on the investigation of the separated information and energy receiver [7], [8], [10], [11], which is based on traditional circuits used for communication and energy harvesting purposes. However, in the seminal contribution in [12], an architecture for the integrated information and energy receiver was proposed. In this architecture, the rectifier that is used for EH is also used for RF band to direct current (DC) conversion, substituting the traditional RF band to baseband conversion. This receiver architecture consumes less power by avoiding the use of active devices, which is particularly important for low power consumption. Moreover, the separated receiver can be combined with the integrated one [13], in order to improve the corresponding symbol error rate at the expense of complexity. Also, the same receiver was considered in the recent contribution in [14], where sequential decoding under fading conditions was proposed aiming at low-complexity detection and efficient memory usage. Likewise, the same receiver architecture was investigated in [15] and a useful metric, namely the joint harvested energy−rate probability, was introduced and defined.

However, despite the importance of [15], its contribution is limited to the analysis of the PS protocol. In other words, it does not investigate the corresponding TS strategy, which exhibits the advantage of simpler implementation compared to the PS counterpart that renders it particularly useful in applications that do not demand continuously active receivers.

978-1-7281-2527-5/19/$31.00 ©2019 IEEE

Motivated by the above, this contribution analyzes a point-to-point TS system and a multicasting TS system consisting of multiple users, where each user is equipped with an integrated receiver. To this end, we first derive a tractable expression for the corresponding achievable rate, which is rather generic as it can be used in various communication scenarios, including the considered point-to-point and multicasting cases. Based on this, we then determine the joint harvested energy−rate outage probability (OP), which was introduced in [15], for both systems and we optimize the TS factor in order to minimize the above probability. Finally, extensive computer simulations present the harvested energy−rate region for a point-to-point TS system and a comparison of the considered systems in terms of the joint harvested energy−rate OP.

II. System Model

We consider the downlink of a communication network, which consists of one base station (BS) that performs SWIPT to serve the assigned EH users. It is assumed that all nodes have a single antenna and each user is equipped with an integrated information and energy receiver [12]. In this context, the analysis focuses on the following two different communication systems: i.) point-to-point communication; ii.) downlink multicasting, where the BS transmits the same information (e.g., a common file) to N users simultaneously. When multiple users are assumed, i.e., in the second system, the notation $(\cdot)_n$ is used to denote the value of the variable $(\cdot)$ for the n-th user. Also, the path loss factor between the BS and the user is denoted by l, while the small scale fading coefficient is given by the complex random variable $h \sim \mathcal{CN}(0,1)$. Finally, we assume that users operate based on the TS protocol.

In the considered integrated receiver, when TS is used the received RF signal is converted to a DC signal by a rectifier consisting of a Schottky diode and a passive low pass filter. This signal is then used for harvesting energy for the portion of time a, whereas for the portion $1-a$ it is used for decoding information, via energy detection. Based on this, the corresponding DC signal is represented as $i_{\text{DC}}(t) = \left||h|\sqrt{lP}A(t) + n_A(t)\right|^2 + n_{\text{rec}}(t)$, where $A(t)$ denotes the amplitude of the complex baseband signal at the transmitter, P denotes the average transmit power, whereas $n_A(t) \sim \mathcal{CN}(0,\sigma_A^2)$ and $n_{\text{rec}} \sim \mathcal{N}(0,\sigma_{\text{rec}}^2)$ denote the normally distributed additive noise introduced by the antenna and the rectifier, respectively.

As shown in [12], the portion of the DC signal for decoding information is processed by an ADC. To this effect, the output of the ADC, $y[k]$, is given by

$$y[k] = \begin{cases} 0, & k \le a, \\ \left||h|\sqrt{lP}A[k]+n_A[k]\right|^2 + n_{\text{rec}}[k]+n_{\text{ADC}}[k], & k > a, \end{cases} \tag{1}$$

where k denotes discrete time and $n_{\text{ADC}} \sim \mathcal{N}(0,\sigma_{\text{ADC}}^2)$ denotes the additive noise introduced by the ADC.

Based on (1) and considering that the antenna noise is negligible, i.e. $\sigma_A^2 \to 0$, the equivalent discrete-time memoryless channel is modeled as $Y = l|h|^2PX + Z$, where X denotes the signal power, which is the non-negative channel input, Y denotes the channel output and $Z \sim \mathcal{N}\left(0, \sigma_{\text{rec}}^2 + \sigma_{\text{ADC}}^2\right)$ denotes the equivalent processing noise. It is also noted that $X \in \mathbb{R}^+$ and $\mathbb{E}[X] \le 1$.

III. Harvested Energy−Rate Trade-off

In what follows, we derive novel expressions for the harvested energy and for the rate of the point-to-point scenario.

A. Harvested Energy

It is assumed that the converted energy in the energy receiver is linearly proportional to i_{DC}, with a conversion efficiency $0 < \zeta \le 1$. It is also assumed that the harvested energy due to the equivalent processing noise is negligible, and thus ignored [12]. Hence, the harvested energy, which coincides with power assuming the symbol period to be one, is given by $Q = a\zeta l|h|^2P$.

B. Achievable Rate

The corresponding achievable rate is derived below.

Theorem 1. *The achievable rate of the considered setup assuming TS is expressed as*

$$R = \frac{1}{2}(1-a)\log_2\left(1 + \frac{e(l|h|^2P)^2}{2\pi(\sigma_{rec}^2 + \sigma_{ADC}^2)}\right) \tag{2}$$

where e represents the Euler's number.

Proof: The channel capacity relates to the mutual information between input and output of the channel through $C \ge I(X,Y)$, where the equality holds for the optimal input distribution. Thus, a capacity lower bound can be obtained using a random input distribution for $X \in \mathbb{R}^+$, $\mathbb{E}[X] \le 1$.

The mutual information between the input and the output of the channel $Y = l|h|^2PX + Z$, can be written as $I(X,Y) = H(Y) - H(Y|X) = H(l|h|^2PX + Z) - H(Z)$, which yields

$$I(X,Y) = \frac{1}{2}\log_2\left(2^{2H(l|h|^2PX+Z)}\right) - H(Z), \tag{3}$$

where $H(\cdot)$ denotes the corresponding information entropy. For the first term in (3), it holds that

$$\frac{1}{2}\log_2\left(2^{2H(l|h|^2PX+Z)}\right) \ge \frac{1}{2}\log_2\left(2^{2H(l|h|^2PX)} + 2^{2H(Z)}\right) \tag{4}$$

and as a result (3) can be re-written as

$$I(X,Y) \ge \frac{1}{2}\log_2\left(1 + \frac{2^{2H(l|h|^2PX)}}{2^{2H(Z)}}\right). \tag{5}$$

Considering that Z follows the normal distribution, the entropy of the equivalent processing noise is expressed as $H(Z) = \log_2\left(2\pi e(\sigma_{\text{rec}}^2 + \sigma_{\text{ADC}}^2)\right)/2$, which yields

$$I(X,Y) \ge \frac{1}{2}\log_2\left(1 + \frac{2^{2H(l|h|^2PX)}}{2\pi e(\sigma_{\text{rec}}^2 + \sigma_{\text{ADC}}^2)}\right) \tag{6}$$

where the exponent in the numerator in (6) is expressed as $H(l|h|^2PX) = H(X) + \log_2(|l|h|^2P|) = H(X) + \log_2(l|h|^2P)$, where l, $|h|^2$ and P are positive constants.

The channel $Y = l|h|^2 PX + Z$, is known as optical intensity channel [16]. It has been shown that a tight lower bound for the capacity of this channel is obtained by mutual information when the input X follows exponential distribution. The rate parameter of the exponential distribution is set to one in order for the restriction $\mathbb{E}[X] \leq 1$ to be satisfied. To this effect, the entropy of X under this distribution is $H(X) = 1/\ln 2$.

Based on (6), the mutual information is computed assuming that the input distribution is exponential. Considering that the portion $1 - a$ is used for decoding information and using the equality, the capacity lower bound is obtained, which is considered as the achievable rate and is given by

$$R = \frac{1}{2}(1-a)\log_2\left(1 + \frac{2^{2(\frac{1}{\ln 2} + \log_2(l|h|^2 P))}}{2\pi e(\sigma^2_{\text{rec}} + \sigma^2_{\text{ADC}})}\right). \quad (7)$$

To this effect, (2) is deduced, which completes the proof. ■

The above theorem is subsequently used in determining the corresponding harvested energy-rate region, which offers useful insights on the behavior of TS based systems.

C. Harvested Energy−Rate Region

Based on Theorem 1 and since $Q = a\zeta l|h|^2 P$, we determine the corresponding harvested energy−rate region for the considered setup. The achievable harvested energy−rate region for the point-to-point system is illustrated in Fig. 1, where the transmit power, the variance of ADC noise and the harvested energy are normalized to the variance of the rectifier noise.

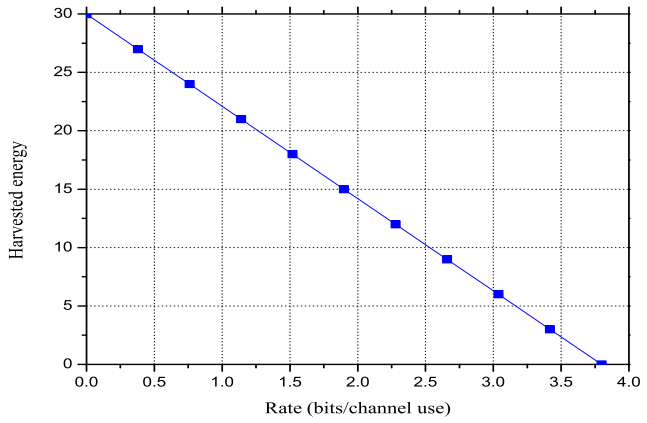

Fig. 1. Harvested energy−rate region with $P = 100$, $h \sim \mathcal{CN}(0,1)$, $\zeta = 0.6$, $l = \frac{1}{2}$, $\sigma^2_{\text{ADC}} = 1$.

IV. Joint Harvested Energy−Rate OP

Capitalizing on the results in Section III, the corresponding joint harvested energy−rate OP is derived.

A. Point-to-Point Communication

The joint harvested energy−rate OP P_o is defined as the probability that the energy harvested by the user is lower than an energy threshold q_{th}, or that the rate is lower than a rate threshold r_{th}. This definition is expressed as

$$P_o = \Pr\left(Q \leq q_{\text{th}} \cup R \leq r_{\text{th}}\right), \quad (8)$$

where $\Pr(\cdot)$ denotes probability.

Theorem 2. *The joint harvested energy−rate OP for a point-to-point system is given by*

$$P_o = 1 - e^{-max\left\{\frac{q_{th}}{a\zeta lP},\ \frac{1}{lP}\sqrt{\frac{2\pi\left(\sigma^2_{rec}+\sigma^2_{ADC}\right)}{e}\left(2^{\frac{2r_{th}}{1-a}}-1\right)}\right\}}, \quad (9)$$

where max$\{\cdot\}$ denotes the maximum of the two elements.

Proof: Based on $Q = a\zeta l|h|^2 P$ and (2), (8) becomes

$$P_o = \Pr\left(a\zeta l|h|^2 P \leq q_{\text{th}} \cup \frac{1-a}{2}\log_2\left(1 + \frac{e(l|h|^2 P)^2}{2\pi\sigma^2}\right) \leq r_{\text{th}}\right), \quad (10)$$

where $\sigma^2 = \sigma^2_{\text{rec}} + \sigma^2_{\text{ADC}}$.

It is recalled that the random variable of both events is $|h|^2$; as a result, it follows that the corresponding OP is given by

$$P_o = \Pr\left(|h|^2 \leq \frac{q_{\text{th}}}{a\zeta lP} \cup |h|^2 \leq \frac{1}{lP}\sqrt{\frac{2\pi\sigma^2}{e}\left(2^{\frac{2r_{\text{th}}}{1-a}}-1\right)}\right). \quad (11)$$

It can be observed that the random variable $|h|^2$ is upper bounded in both events. The union of these events occurs when $|h|^2$ is lower than the maximum of these upper bounds. Hence, P_o can be expressed as

$$P_o = \Pr\left(|h|^2 \leq \max\left\{\frac{q_{\text{th}}}{a\zeta lP},\ \frac{1}{lP}\sqrt{\frac{2\pi\sigma^2}{e}\left(2^{\frac{2r_{\text{th}}}{1-a}}-1\right)}\right\}\right). \quad (12)$$

It is recalled that $h \sim \mathcal{CN}(0,1)$; consequently, $|h|$ follows a Rayleigh distribution with scale parameter $\sqrt{2}/2$ and $|h|^2$ follows an exponential distribution with rate parameter 1. The probability density function (PDF) for this distribution is $f(x) = e^{-x}$ and the corresponding OP is expressed as

$$P_o = \int_0^{\max\left\{\frac{q_{\text{th}}}{a\zeta lP},\ \frac{1}{lP}\sqrt{\frac{2\pi\left(\sigma^2_{\text{rec}}+\sigma^2_{\text{ADC}}\right)}{e}\left(2^{\frac{2r_{\text{th}}}{1-a}}-1\right)}\right\}} e^{-x}dx. \quad (13)$$

Based on the above and after some algebraic manipulations, equation (9) is deduced, which completes the proof. ■

Of note, one of the main aims in SWIPT systems is to minimize the OP. Hence, the optimal value of a is defined as

$$a^* = \arg\min_a P_o. \quad (14)$$

Proposition 1. *The optimal value of $a \in [0,1]$ is given by*

$$a^2\left(2^{\frac{2r_{th}}{1-a}}-1\right) - \frac{q^2_{th}e}{2\pi\zeta^2(\sigma^2_{rec}+\sigma^2_{ADC})} = 0. \quad (15)$$

Proof: As the PS factor ρ increases, the first term in

$$\max\left\{\frac{q_{\text{th}}}{a\zeta lP},\ \frac{1}{lP}\sqrt{\frac{2\pi\left(\sigma^2_{\text{rec}}+\sigma^2_{\text{ADC}}\right)}{e}\left(2^{\frac{2r_{\text{th}}}{1-a}}-1\right)}\right\}$$

decreases, whereas the second term increases. Therefore, the probability is minimized when the above maximal value is minimized; that is, the two terms are equal and the optimal TS factor can be extracted from

$$\frac{q^2_{\text{th}}}{a^2\zeta^2} = \frac{2\pi\left(\sigma^2_{\text{rec}}+\sigma^2_{\text{ADC}}\right)}{e}\left(2^{\frac{2r_{\text{th}}}{1-a}}-1\right). \quad (16)$$

Based on (16) and after some mathematical manipulations, (15) can be derived. Also, the solution is guaranteed to be in the interval; this is because for $a = 0$ the first term is infinite, whereas for $\rho = 1$ the second term is infinite. ■

B. Downlink Multicasting

In a downlink multicasting TS system and recalling that $Q = a\zeta l|h|^2 P$, the harvested energy by the n-th user is given by $Q_n = a_n \zeta_n l_n |h_n|^2 P$. Accordingly, with the aid of (2), the rate of the n-th user is expressed as

$$R_n = \frac{1}{2}(1 - a_n) \log_2 \left(1 + \frac{e(l_n |h_n|^2 P)^2}{2\pi \left(\sigma^2_{\text{rec,n}} + \sigma^2_{\text{ADC,n}} \right)} \right). \quad (17)$$

Theorem 3. *The joint harvested energy−rate OP for a multicasting system, which is defined as the probability that at least one user is in outage, is given by*

$$P_o = 1 - \prod_{n=1}^{N} e^{-max\left\{ \frac{q_{th,n}}{a_n \zeta_n l_n P}, \frac{1}{l_n P} \sqrt{\frac{2\pi \left(\sigma^2_{rec,n} + \sigma^2_{ADC,n} \right)}{e}} \left(2^{\frac{2r_{th}}{1-a_n}} - 1 \right) \right\}}. \quad (18)$$

Proof: The joint harvested energy−rate OP can be expressed as $P_o = \Pr\left(Q_1 \leq q_{\text{th,1}} \cup R_1 \leq r_{\text{th}} \cup \cdots \cup Q_N \leq q_{\text{th,N}} \cup R_N \leq r_{\text{th}}\right)$. It is noted here that the threshold of harvested energy can be practically different in each user; however, the same does not hold for the rate, due to the multicasting principle. Hence, exploiting the complementary event and since $|h_n|^2$ are statistically independent $\forall n \in \{1, ..., N\}$, it follows that $P_o = 1 - \prod_{n=1}^{N} \Pr\left(Q_n \leq q_{\text{th,n}} \cup R_n \leq r_{\text{th}}\right)$. Hence, the joint harvested energy−rate OP for a multicasting system is obtained by (18), which completes the proof. ■

It is recalled that the optimal TS factor for each user can be determined with the aid of Proposition 1.

V. Results and Discussion

In this section, we use the offered analytical and simulation results to quantify the performance and characteristics of the considered set up. To this end, it is assumed that the transmit power, the variance of ADC noise and the harvested energy are normalized to the variance of the rectifier noise. Without loss of generality and unless stated otherwise, it is also assumed that $P = 100$, $\sigma^2_{\text{ADC}} = 1$ and $\zeta = 0.6$ [12], whereas the distance for all users is considered $d = 1$m. Also, in all figures, the values of ρ and a are optimally selected. Moreover, the path loss factor is given by the bounded model [8], [10], i.e., $l = 1/(1 + d^a)$, where $a = 2$ denotes the path loss exponent.

In Fig. 2, a point-to-point system, a multicasting system of 2 users and a multicasting system of 3 users are demonstrated for a harvested energy threshold $q_{\text{th}} = 5$ and a rate threshold $r_{\text{th}} = 1$ bits/channel use. The joint harvested energy−rate OPs of the three systems are compared, when the distance of one of the users increases. It is observed that in long distances, the number of users has limited effect on the overall system performance. Likewise, Fig. 3 demonstrates the joint harvested energy−rate OP of the same systems against the transmit power, with $q_{\text{th}} = 5$ and $r_{\text{th}} = 1$ bits/channel use. It is evident that the performance of point-to-point systems outperforms the performance of the multicasting counterparts for two and three users, particularly at low transmit power values. On the contrary, as the transmit power increases, the achieved performance tends to converge. However, it is evident that the corresponding performance improvement exhibits saturation in terms of increasing transmit power. This verifies the criticality of selecting the number of users based on the system parameters, since it is not practically effective to assume that performance compensations can be achieved by simply increasing the transmit power.

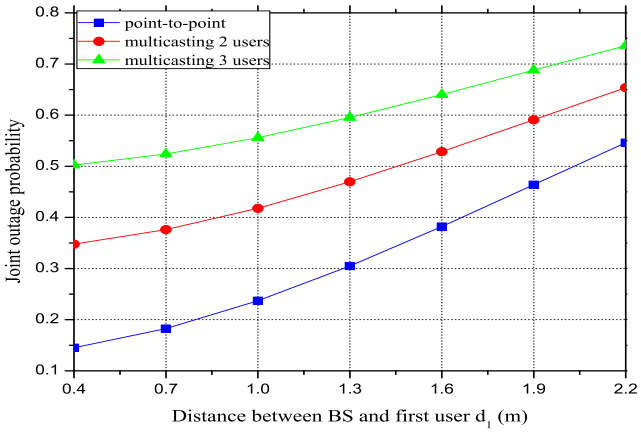

Fig. 2. OP versus distance d_1.

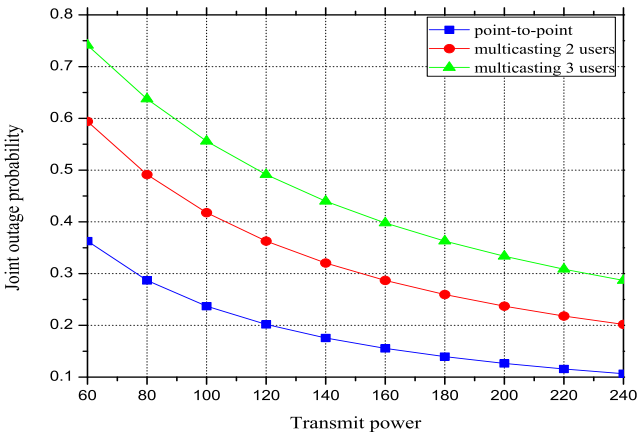

Fig. 3. OP versus transmit power.

Figs. 4 and 5 illustrate the effect of both thresholds for harvested energy and achievable rate on the joint OP and the optimal selection of a in the case of a point-to-point system. It is evident that as the thresholds increase, the joint OP also increases, whereas the optimal TS factor increases when the energy threshold increases or the rate threshold decreases. Furthermore, it is observed that $a^* \in [0, 1]$ spans a large range of values for different thresholds. Finally, a similar trend is observed for the case of a multicasting system consisting of two users, the performance of which is illustrated in Fig. 6.

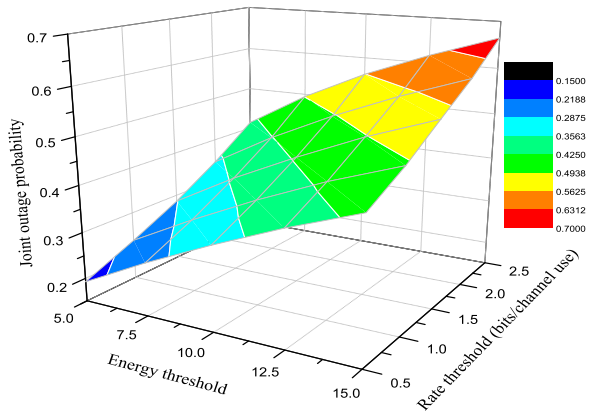

Fig. 4. OP versus energy and rate thresholds in a point-to-point system.

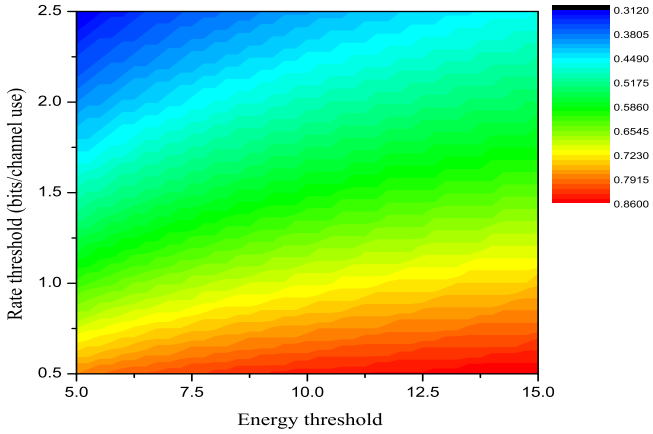

Fig. 5. Optimal TS factor versus energy and rate thresholds in a point-to-point system.

VI. Conclusions

This work investigated the performance of the integrated energy and information receiver. The trade-off between the harvested energy and the rate has been quantified when TS strategy is assumed. In order to balance the trade-off between the harvested energy and the rate in a point-to-point and in a multicasting system, the joint harvested energy−rate OP is introduced and minimized. Also, the ADC noise has been considered, which has a critical impact on the optimal selection of the TS factor. The offered results showed that this receiver can be used in systems consisting of multiple users where high energy efficiency and low-complexity at the users' side are of greater importance than high data rates.

Acknowledgment

This work was supported in part by Khalifa University under Grants KU/RC1-C2PS-T2/8474000137 and KU/FSU-8474000122.

References

[1] I. Krikidis, S. Timotheou, S. Nikolaou, G. Zheng, D. W. K. Ng, and R. Schober, "Simultaneous wireless information and power transfer in modern communication systems," *IEEE Commun. Mag.*, vol. 52, no. 11, pp. 104–110, Nov. 2014.

[2] P. Grover and A. Sahai, "Shannon meets Tesla: Wireless information and power transfer," in *Proc. IEEE ISIT '10*, Jun. 2010, pp. 2363–2367.

[3] Y. Liu, L. Wang, M. Elkashlan, T. Q. Duong, and A. Nallanathan, "Two-way relaying networks with wireless power transfer: Policies design and throughput analysis," in *IEEE GLOBECOM '14*, IEEE, 2014, pp. 4030–4035.

[4] S. Bi, C. K. Ho, and R. Zhang, "Wireless powered communication: Opportunities and challenges," *IEEE Commun. Mag.*, vol. 53, no. 4, pp. 117–125, Apr. 2015.

[5] R. Zhang and C. K. Ho, "MIMO Broadcasting for Simultaneous Wireless Information and Power Transfer," *IEEE Trans. Wireless Commun.*, vol. 12, no. 5, pp. 1989–2001, May 2013.

[6] Z. Ding, C. Zhong, D. W. K. Ng, M. Peng, H. A. Suraweera, R. Schober, and H. V. Poor, "Application of smart antenna technologies in simultaneous wireless information and power transfer," *IEEE Commun. Mag.*, vol. 53, no. 4, pp. 86–93, Apr. 2015.

[7] D. W. K. Ng, E. S. Lo, and R. Schober, "Energy-efficient power allocation in OFDM systems with wireless information and power transfer," in *Proc. IEEE ICC '13*, Jun. 2013, pp. 4125–4130.

[8] Z. Ding, I. Krikidis, B. Sharif, and H. V. Poor, "Wireless information and power transfer in cooperative networks with spatially random relays," *IEEE Trans. Wirel. Commun.*, vol. 13, no. 8, pp. 4440–4453, Aug. 2014.

[9] H. Xing, L. Liu, and R. Zhang, "Secrecy wireless information and power transfer in fading wiretap channel," *IEEE Trans. Veh. Technol.*, vol. 65, no. 1, pp. 180–190, Jan. 2016.

[10] P. D. Diamantoulakis, G. D. Ntouni, K. N. Pappi, G. K. Karagiannidis, and B. S. Sharif, "Throughput maximization in multicarrier wireless powered relaying networks," *IEEE Wireless Commun. Lett.*, vol. 4, no. 4, pp. 385–388, Aug. 2015.

[11] Q. Wu, M. Tao, D. W. K. Ng, W. Chen, and R. Schober, "Energy-efficient resource allocation for wireless powered communication networks," *IEEE Trans. Wirel. Commun.*, vol. 15, no. 3, pp. 2312–2327, Mar. 2016.

[12] X. Zhou, R. Zhang, and C. K. Ho, "Wireless information and power transfer: Architecture design and rate-energy tradeoff," *IEEE Trans. Commun.*, vol. 61, no. 11, pp. 4754–4767, Nov. 2013.

[13] C. H. Chang, R. Y. Chang, and F. T. Chien, "Energy-assisted information detection for simultaneous wireless information and power transfer: Performance analysis and case studies," *IEEE Trans. Signal Inf. Process. Netw.*, vol. 2, no. 2, pp. 149–159, Jun. 2016.

[14] E. Goudeli, C. Psomas, and I. Krikidis, "Sequential decoding for simultaneous wireless information and power transfer," in *24th ICT '14*. IEEE, May 2017, pp. 1–5.

[15] S. A. Tegos, P. D. Diamantoulakis, K. Pappi, and G. K. Karagiannidis, "Optimal simultaneous wireless information and power transfer with low-complexity receivers," in *IEEE SPAWC '18*. IEEE, 2018, pp. 1–5.

[16] A. Lapidoth, S. M. Moser, and M. A. Wigger, "On the capacity of free-space optical intensity channels," *IEEE Trans. Inf. Theory*, vol. 55, no. 10, pp. 4449–4461, Oct. 2009.

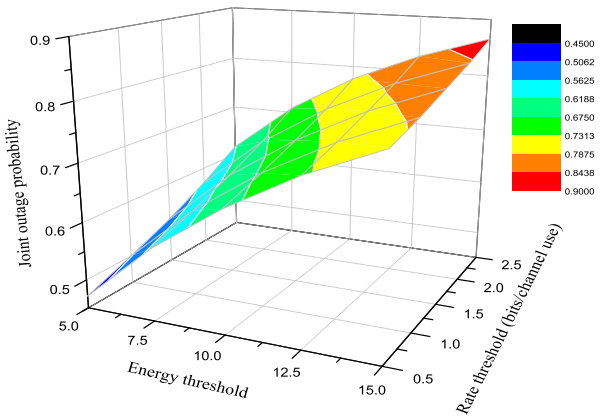

Fig. 6. OP versus energy and rate thresholds in a multicasting system.